Mass spectra and decay of mesons under strong external magnetic field*

Shuyun Yang(杨淑芸)† Meng Jin(金猛)‡ Defu Hou(侯德富)§

Institute of Particle Physics and Key Laboratory of Quark and Lepton Physics (MOS), Central China Normal University, Wuhan 430079, China

Abstract: We study the mass spectra and decay process of σ and π_0 mesons under a strong external magnetic field. To achieve this goal, we deduce the thermodynamic potential in a two-flavor, hot and magnetized Nambu–Jona-Lasinio model. We calculate the energy gap equation through the random phase approximation (RPA). Then we use the Ritus method to calculate the decay triangle diagram and self-energy in the presence of a constant magnetic field B. Our results indicate that the magnetic field has little influence on the mass of π_0 at low temperatures. However, for quarks and σ mesons, their mass clearly changes, which reflects the influence of magnetic catalysis (MC). The presence of a magnetic field accelerates the decay of the meson while the presence of a chemical potential will decrease the decay process.

Keywords: magnetic field, NJL model, decay constant, mass spectra

DOI: 10.1088/1674-1137/ac4694

I. INTRODUCTION

Over the years, studies on the nature and state of strong interacting substances under extreme conditions have attracted much attention, where extreme conditions include high temperature and finite baryon chemical potential [1-3], as well as strong magnetic fields. In this paper we discuss the effects of finite magnetic fields on strong interacting matter [4-14]. Magnetic field changes are closely related to high-energy nuclear collisions, dense stars and cosmic phase transitions. The maximum magnetic field observed in nature is about 10^{12}–10^{13} Gauss in pulsars, the maximum magnetic field on the surface of some magnetospheric stars is around $10^{14}-10^{15}$ Gauss, and its internal field is estimated to be $10^{18}-10^{20}$ Gauss. In the early stage of the RHIC noncentral heavy ion collision, there is also an evidence of a very strong and instantaneous magnetic field. Depending on the energy of the collision and impact parameters, the magnetic field produced in RHIC is about $eB\sim 1.5m_\pi^2\sim 0.03$ GeV^2, and $eB\sim 15m_\pi^2\sim 0.3$ GeV^2 in the LHC [15-18]. On the other hand, the quark–gluon plasma produced in high energy heavy-ion collisions went through many stages in the process of evolution. A large number of hadrons including π are produced, freeze out and then survive in the final state [19]. Therefore, the existence of the background magnetic field generated in the heavy ion experiment may affect the properties of the early "charged quarks" in the collision. Although this strong magnetic field lasts a very short time and disappears very fast, it may affect the properties of the hadrons formed by these "magnetized" quarks. Even the properties of neutral mesons may be affected by external magnetic fields produced in the early stage of heavy ion collisions [16, 17].

This paper is based on the two-flavor NJL model [20-23]. We calculate the energy gap equation by the mean field approximation. We use the Ritus method to calculate the decay triangle diagram and self-energy in the magnetic field through Random Phase Approximation (RPA), then we obtain the meson decay width and meson–quark coupling constant. Our result shows that as quarks which constitutes mesons are magnetized under a magnetic field, the mass of σ grows, whereas the mass of π_0 changes very little at low temperature, and the coupling constants $g_{\sigma qq}$ and $g_{\pi_0 qq}$ are significantly larger than that without a magnetic field.

The organization of the paper is as follows. In Sec. II, we give the effective thermodynamic potential. In Sec. III, we calculate the mass spectra of mesons and the decay constant of $\sigma\to\pi_0\pi_0$. Section IV gives the numerical results of our work. Finally we summarize and discuss

Received 19 December 2021; Accepted 29 December 2021; Published online 1 March 2022

* Supported by the National Natural Science Foundation of China (11735007, 11890711, 11890710)

† E-mail: yangsy@mails.ccnu.edu.cn

‡ E-mail: jinmeng@mail.ccnu.edu.cn

§ E-mail: houdf@mail.ccnu.edu.cn

some possible extension of our work in Sec. V.

II. EFFECTIVE THERMODYNAMIC POTENTIAL

The Lagrangian density of the $SU(2)$ NJL model is

$$\mathcal{L}_{\rm NJL}=\bar{\psi}({\rm i}\gamma^{\mu}\partial_{\mu}-m_0)\psi+G[(\bar{\psi}\psi)^2+(\bar{\psi}{\rm i}\gamma_5\boldsymbol{\tau}\psi)^2]. \tag{1}$$

The Lagrangian density has $SU_V(2)\times SU_A(2)\times U_V(1)$ symmetry, where $SU_V(2)$ corresponds to the chiral symmetry, $SU_A(2)$ corresponds to the conservation of isotopic spin, and $U_V(1)$ corresponds to the conservation of baryon numbers. In the formula, ψ and $\bar{\psi}$ are quark fields. When the isospin symmetry is satisfied, we have $m_{\mu}=m_d=m_0$. $D^{\mu}=\partial^{\mu}+{\rm i}eA^{\mu}$ is covariant differentiation, $A^{\mu}=\delta^{\mu}_0A^0$ and $A^0=-{\rm i}A^4$ are gauge fields. G is the four-quark coupling constant. The Pauli matrix $\tau_i(i=1,2,3)$ is defined in the isospin space.

The thermodynamic potential can be expressed as

$$\Omega=-\frac{T}{V}\ln Z, \tag{2}$$

with the partition function

$$Z(T,\mu,V)=\int[{\rm d}\bar{\psi}][{\rm d}\psi]{\rm e}^{\int_0^{\beta}{\rm d}\tau\int{\rm d}^3\boldsymbol{x}(\mathcal{L}+\bar{\psi}\mu\gamma_0\psi)}, \tag{3}$$

where V is the volume, $\beta=\frac{1}{T}$. $\mu={\rm dig}(\mu_u,\mu_d)$ is the chemical potential of the quark. Following the calculations such as [24, 25], we have the thermodynamic potential under the mean field approximation,

$$\begin{aligned}\Omega=&-\frac{T}{V}\ln Z=-\frac{T}{V}\ln{\rm Tr}{\rm e}^{-\beta\int{\rm d}^3\boldsymbol{x}(\mathcal{L}+\bar{\psi}\mu\gamma_0\psi)}\\=&\Omega_q+\frac{(m_q-m_0)^2}{4G}+{\rm const}.\end{aligned} \tag{4}$$

where Ω_q is the contribution of the quark part

$$\Omega_q(T,\mu)=-T\sum_n\int\frac{{\rm d}^3\boldsymbol{p}}{(2\pi)^3}{\rm Tr}\ln\left(\beta S^{-1}({\rm i}\omega_n,\boldsymbol{p})\right). \tag{5}$$

In this formula $S^{-1}(p)=\gamma^{\mu}p_{\mu}-m_q$, $p^0={\rm i}\omega_n=(2n+1)\pi T$. It is known that

$${\rm Tr}\ln(\gamma^{\mu}p_{\mu}-m_q)=\ln{\rm Det}(\gamma^{\mu}p_{\mu}-m_q)=2N_cN_f\ln(p^2-m_q^2). \tag{6}$$

Using of the summation formula [26]

$$T\sum_n\ln(\beta^2(\omega_n^2+\lambda_k^2))=\lambda_k+2T\ln(1+{\rm e}^{-\beta\lambda_k}), \tag{7}$$

one can obtain

$$\begin{aligned}\Omega_q(T,\mu)=&-2N_cN_f\int\int\frac{{\rm d}^3\boldsymbol{p}}{(2\pi)^3}\{E_p+T\ln(1+{\rm e}^{-\beta(E_p-\mu)}\\&+T\ln(1+{\rm e}^{-\beta(E_p+\mu)})\}.\end{aligned} \tag{8}$$

where, $E_p=\sqrt{p_3^2+m_q^2}$. Regardless of the chemical potential, $\mu=0$, the formula will change to

$$\Omega_q=-2N_cN_f\int\frac{{\rm d}^3\boldsymbol{p}}{(2\pi)^3}\{E_p+2T\ln(1+{\rm e}^{-\beta E_p})\}. \tag{9}$$

If the magnetic field is added, one will find that

$$2N_f\int\frac{{\rm d}^3\boldsymbol{p}}{(2\pi)^3}\to\sum_{f,n}\alpha_n\frac{|Q_fB|}{2\pi}\int\frac{{\rm d}p_3}{2\pi}, \tag{10}$$

then, the thermodynamic potential becomes

$$\begin{aligned}\Omega_q(T,\mu)=&-N_c\sum_{f,n}\alpha_n\frac{|Q_fB|}{2\pi}\int\frac{{\rm d}p_3}{2\pi}\{E_f+T\ln\left(1+{\rm e}^{-\beta(E_f-\mu)}\right)\\&+T\ln\left(1+{\rm e}^{-\beta(E_f+\mu)}\right)\}.\end{aligned} \tag{11}$$

where, $E_f=\sqrt{p_3^2+2n|Q_fB|+m_q^2}$, $\alpha_n=2-\delta_{n0}$, charge $Q={\rm diag}(Q_u,Q_d)$ to the external magnetic field $\boldsymbol{B}=(0,0,B)$ in z-direction, f is flavor u or d.

III. DECAY PROCESS IN TWO-FLAVOR NJL MODEL

The energy gap equation can be derived from the derivative of the thermodynamic potential. From the energy gap equation we can calculate the mass of the quark and the single-loop self-energy through RPA [21-23, 27] in a two-flavor NJL model. As for the selection of magnetical quark propagators, usually we have two methods: Ritus scheme [18, 28-36] and the Schwinger scheme [11, 12]. In this paper, the Ritus scheme is used to deal with propagators, which is described in coordinate space,

$$S_f(x,y)=\sum_n\int\frac{{\rm d}^3\tilde{p}}{(2\pi)^3}{\rm e}^{-{\rm i}\tilde{p}(x-y)}P_n(x_1,p_2)D_f(\bar{p})P_n(y_1,p_2), \tag{12}$$

where,

$$D_f(\bar{p})=\gamma\cdot\bar{p}-m_q, \tag{13}$$

and the magnetic field related terms are

$$P_n(x_1,p_2)=\frac{1}{2}\left[g_n^{sf}(x_1,p_2)+I_n g_{n-1}^{sf}(x_1,p_2)\right] + \frac{\mathrm{i}S_f}{2}\left[g_n^{sf}(x_1,p_2)-I_n g_{n-1}^{sf}(x_1,p_2)\right]\gamma_1\gamma_2, \quad (14)$$

the term $g_n^{sf}(x_1,p_2)=\phi_n(x_1-s_f p_2/|Q_f B|)$ is determined by hermite polynomial $H_n(\zeta)$.

$$\phi_n(\zeta)=\left(2^n n!\sqrt{\pi}|Q_f B|^{-1/2}\right)^{-\frac{1}{2}}\mathrm{e}^{-\frac{\zeta^2|Q_f B|}{2}}H_n\left(\zeta/|Q_f B|^{-1/2}\right). \quad (15)$$

Here, $\tilde{p}=(p_0,0,p_2,p_3)$ is the momentum of the Fourier transform, and $\bar{p}=(p_0,0,-s_f\sqrt{2n|Q_f B|},p_3)$ is the conserved Ritus momentum. $s_f=sgn(Q_f B)$, $Q_f=(2/3,-1/3)$, and f means quark flavor. $I_n=1-\delta_{n0}$, where n is the landau energy level.

A. Mass spectra of mesons

To illustrate the Ritus scenario clearly, we use neutral mesons as a simple example. In this case, the meson momentum $k=(\omega,k_1,k_2,k_3)$ is conserved for neutral mesons which do not interact with the magnetic field. The corresponding meson polarization functions in the momentum space are the Fourier transforms of their expressions in the coordinate space,

$$\mathcal{D}_M(k)=\int \mathrm{d}^4(x-y)\mathrm{e}^{\mathrm{i}k(x-y)}\mathcal{D}_M(x,y),$$
$$\Pi_M(k)=\int \mathrm{d}^4(x-y)\mathrm{e}^{\mathrm{i}k(x-y)}\Pi_M(x,y). \quad (16)$$

Using random phase approximation, one can obtain

$$\mathcal{D}_M(k)=\frac{2G}{1-2G\Pi_M(k)}. \quad (17)$$

The mass of a meson is defined by the pole of the denominator at zero momentum

$$1-2G\Pi_M(\omega=m_M,\mathbf{0})=0. \quad (18)$$

The polarization function is [37],

$$\Pi_M(\omega,\mathbf{0})=J_1-(\omega^2-\epsilon_M^2)J_2(\omega^2), \quad (19)$$

where,

$$J_1=2N_c N_f\int\frac{\mathrm{d}^3\boldsymbol{p}}{(2\pi)^3}\frac{\tanh\left(\frac{E_f}{2T}\right)}{E_f}, \quad (20)$$

and

$$J_2(\omega^2)=-2N_c N_f\int\frac{\mathrm{d}^3\boldsymbol{p}}{(2\pi)^3}\frac{\tanh\left(\frac{E_f}{2T}\right)}{E_f(4E_f^2-w^2)}, \quad (21)$$

with $\epsilon_{\pi_0}=0$ and $\epsilon_\sigma=2m_q$.

Under zero magnetic field

$$\Pi_M(\omega,\mathbf{0})=2N_c N_f\int\frac{\mathrm{d}^3\boldsymbol{p}}{(2\pi)^2}\frac{E_f-\epsilon_M^2}{E_f^2-\frac{w^2}{4}}\left(1-2f_F(E_f)\right), \quad (22)$$

where $E_f=\sqrt{\boldsymbol{p}^2+m_q^2}$ for the distribution function $f_F(E_f)=\frac{1}{\mathrm{e}^{\beta E_f+1}}$. After considering the magnetic field, one can make the substitution in Eq. (11). Therefore, the self-energy of mesons under external magnetic field can be further obtained,

$$\Pi_M'(\omega,\mathbf{0})=N_c\sum_{f,n}\alpha_n\frac{|Q_f B|}{2\pi}\int\frac{\mathrm{d}p_3}{2\pi} \times\frac{1-f_F\left(E_f-\mu\right)-f_F\left(E_f+\mu\right)}{E_f} + (\omega^2-\epsilon_M^2)N_c\sum_{f,n}\alpha_n\frac{|Q_f B|}{2\pi}\int\frac{\mathrm{d}p_3}{2\pi} \times\frac{1-f_F\left(E_f-\mu\right)-f_F\left(E_f+\mu\right)}{E_f\left(4E_f^2-w^2\right)}. \quad (23)$$

B. Decay rate for $\sigma\to\pi_0\pi_0$

Elementary particles have the tendency to decay. For a given interaction, the larger the mass difference between the initial particles and the decay products, the faster the decay proceeds. Here we define the decay rate for $\sigma\to\pi_0\pi_0$ at the one-loop level depicted in Fig. 1 by a Lorentz conservation matrix M [38]

$$\frac{\mathrm{d}\Gamma_{\sigma\to2\pi_0}}{\mathrm{d}\Omega}=\frac{1}{32\pi^2}\frac{|P|}{m_\sigma^2}\left|M(T,\mu)\right|^2, \quad (24)$$

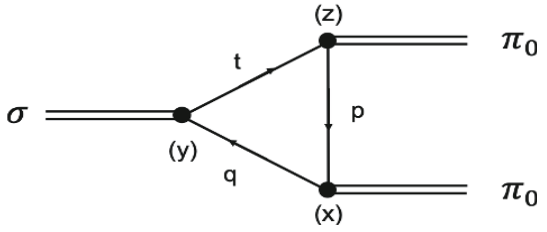

Fig. 1. Feynman diagram for the process $\sigma\to\pi_0\pi_0$.

where π_0 momentum is $|P|=\sqrt{\frac{m_\sigma^2}{4}-m_{\pi_0}^2}$ and $M(T,\mu)=g_\sigma g_{\pi_0}^2 A_{\sigma\pi_0\pi_0}$.

At a finite temperature and density, the decay rate of $\sigma\to\pi\pi$ process is [39]

$$\Gamma_{\sigma\to2\pi_0}(T,\mu)=\Gamma_{\sigma\to2\pi_0}(T,\mu)=\frac{3}{8\pi}\frac{\sqrt{m_\sigma^2/4-m_{\pi_0}^2}}{m_\sigma^2}g_\sigma^2 g_{\pi_0}^4 \times\left|A_{\sigma\pi_0\pi_0}(T,\mu)\right|^2\left[1+2f_{\rm B}\left(\frac{m_\sigma}{2}\right)\right]. \tag{25}$$

where $f_{\rm B}(m_\sigma/2)=1/(\mathrm{e}^{\frac{m_\sigma}{2}}-1)$ is the Bose–Einstein distribution function.

σ coupling constant and π coupling constant are respectively defined by

$$g_{\sigma qq}^{-2}=\frac{\partial\Pi_\sigma(k_0,\boldsymbol{0})}{\partial k_0^2},\qquad g_{\pi_0qq}^{-2}=\frac{\partial\Pi_{\pi_0}(k_0,\boldsymbol{0})}{\partial k_0^2}. \tag{26}$$

The triangle factor $A_{\sigma\pi_0\pi_0}$ is defined by

$$\mathrm{i}A_{\sigma\pi_0\pi_0}(T,\mu)=-T_r\int\frac{\mathrm{d}^4q}{(2\pi)^4}\left[g_{\sigma qq}\Gamma_\sigma \mathrm{i}S_u(x,y)g_{\pi_0qq}\times\Gamma_\pi \mathrm{i}S_u(y,z)g_{\pi_0qq}\Gamma_\pi \mathrm{i}S_u(z,x)\right]. \tag{27}$$

The vertex of the meson is expressed as

$$\Gamma_M=\begin{cases}1 & M=\sigma,\\ \mathrm{i}\tau_3\gamma_5 & M=\pi_0.\end{cases} \tag{28}$$

In Eq. (12), we have defined the propagator of meson in coordinate space. Here, we let

$$\begin{aligned}P_n(x_1,q_2)=&\frac{1}{2}\left[g_n^{S_f}(x_1,q_2)+I_n g_{n-1}^{S_f}(x_1,q_2)\right]\\&+\frac{\mathrm{i}S_f}{2}\left[g_n^{S_f}(x_1,q_2)-I_n g_{n-1}^{S_f}(x_1,q_2)\right]\gamma_1\gamma_2\\=&\frac{1}{2}\left[f_{k+}(x)+f_{k-}(x)\right]+\frac{\mathrm{i}S_f}{2}\left[f_{k+}(x)-f_{k-}(x)\right]\gamma_1\gamma_2\\=&A_x+\mathrm{i}S_f B_x\gamma_1\gamma_2.\end{aligned} \tag{29}$$

Then, we can obtain the triangle factor $A_{\sigma\pi_0\pi_0}$

$$\begin{aligned}A_{\sigma\pi_0\pi_0}(x,y,z)=&2\mathrm{i}^6N_c g_{\sigma qq}g_{\pi_0qq}^2\,\mathrm{Tr}\left[1\cdot S_u(x,y)\cdot r_5\cdot S_u(y,z)\cdot r_5\cdot S_u(z,x)\right]=2\mathrm{i}^2N_c g_{\sigma qq}g_{\pi_0qq}^2\sum_{n,n',n''}\int\frac{\mathrm{d}^3\tilde{p}\mathrm{d}^3\tilde{q}^3\tilde{q}}{(2\pi)^9}\mathrm{e}^{-\mathrm{i}\tilde{q}(x-y)-\mathrm{i}\tilde{l}(y-z)-\mathrm{i}\tilde{p}(z-x)}\\&\times\mathrm{Tr}\left[P_n(x_1,q_2)\frac{r\cdot\bar{q}+m_q}{\bar{q}^2-m_q^2}P_n(y,q_2)\cdot P_{n'}(y_1,t_2)\frac{-r\cdot\bar{l}+m_q}{\bar{q}^2-m_q^2}P_{n'}(z_1,t_2)\cdot P_{n''}(z_1,p_2)\frac{r\cdot\bar{p}+m_q}{\bar{q}^2-m_q^2}P_n''(x_1,p_2)\right].\end{aligned} \tag{30}$$

Normalization was carried out using the following formula [33]

$$\begin{cases}\int \mathrm{d}x f_{k+}(x)f_{l+}(x)=\delta_{k,l}\Longrightarrow f_{k+}f_{k+} & \text{remain},\\ \int \mathrm{d}x f_{k+}(x)f_{l-}(x)=\delta_{k,l-1}(l\geq1)\Longrightarrow f_{k+}f_{k-}=0,\\ \int \mathrm{d}x f_{k-}(x)f_{l-}(x)=\delta_{k,l}\Longrightarrow f_{k-}f_{k-} & \text{ramain},\\ \int \mathrm{d}x f_{k-}(x)f_{l+}(x)=\delta_{k-1,l}(k\geq1)\Longrightarrow f_{k-}f_{k+}=0,\end{cases} \tag{31}$$

and $\mathrm{e}^{-\mathrm{i}\widetilde{q}(x-y)-\mathrm{i}\widetilde{l}(y-z)-\mathrm{i}\widetilde{p}(z-x)}$ in coordinate space can be changed to $(\bar{k},\bar{p}_3)$ momentum space by Fourier transform. For $y-z\neq0$ and $z-x\neq0$, the relationship of momentum conservation becomes

$$\widetilde{l}=\widetilde{q}+\widetilde{k},\qquad \widetilde{p}=\widetilde{q}+\widetilde{p}_3\ . \tag{32}$$

Finally, we have the triangle factor

$$\begin{aligned}A_{\sigma\pi_0\pi_0}(k,p_3)=&2mg_{\sigma qq}g_{\pi_0qq}^2N_c\sum_{f,n}\alpha_n\frac{|Q_fB|}{2\pi}\int\frac{\mathrm{d}q_3}{2\pi}\\&\times\frac{f_F\left(E_q-\mu\right)-f_F\left(-E_q-\mu\right)}{2E_q}\\&\times\frac{\frac{S^2}{2}-2SE_q^2-\left(4m_\pi^2+2S\right)\boldsymbol{q}\cdot\boldsymbol{p_3}+8(\boldsymbol{q}\cdot\boldsymbol{p_3})^2}{\left(S-4E_q^2\right)\left[\left(m_\pi^2-2\boldsymbol{q}\cdot\boldsymbol{p_3}\right)^2-SE_q^2\right]},\end{aligned} \tag{33}$$

where $S=m_\sigma^2$, $|\boldsymbol{p_3}|=\sqrt{m_\sigma^2/4-m_{\pi_0}^2}$, $|\boldsymbol{q}|=\sqrt{q_3^2+2n|Q_feB|}$. Since we only consider the decay process of $\sigma\to\pi_0\pi_0$, the decay constant can be approximated as

$$\Gamma_{\sigma\to\pi_0\pi_0}(T,\mu)=\frac{3}{8\pi}\frac{\sqrt{m_\sigma^2/4-m_{\pi_0}^2}}{m_\sigma^2}g_{\sigma qq}^2g_{\pi_0qq}^4 \times\left|A_{\sigma\pi_0\pi_0}(T,\mu)\right|^2\left[1+2f_{\rm B}\left(\frac{m_\sigma}{2}\right)\right]. \tag{34}$$

IV. NUMERICAL RESULTS

The chiral condensate or the dynamical quark mass is controlled by the minimum of the thermodynamic potential [11, 12, 36, 40, 41]. Using the thermodynamic potential from Eq. (11), we have

$$\frac{\partial \Omega_{mf}}{\partial m_q} = 0. \tag{35}$$

In this work, our choice of parameters are $m_0 = 5$ MeV, $\Lambda = 653.3$ MeV, $G = 4.93\times10^{-6}$ MeV^2. The hard-cutoff regularization scheme is adopted to deal with the integral in our work. There are other kinds of regularization schemes, such as soft-cutoff regularization scheme and Pauli–Villars regularization scheme; one may find these methods in Ref. [42].

The diagrams of mass variation corresponding to the temperature under different external magnetic fields $eB = 0,2,5,7m_\pi^2$ are plotted in Fig. 2. We observe that when the temperature increases, the mass of the quark decreases first slowly then sharply, and finally changes slowly after $T = 200$ MeV. For a fixed temperature, the quark mass gradually increases with the increase of magnetic field.

Figure 2 indicates that with the increase of magnetic field, the temperature when the chiral symmetry is restored increases continuously. This temperature is the so-called critical temperature T_C. We plot black points in Fig. 2 and Fig. 3, which means that at this point, the chiral symmetry is restored. The temperature of this point is the critical temperature of the chiral phase transition T_C.

When $m_\pi = 2m_q$, the temperature is the Mott temperature [5, 36], $T_{\rm Mott}$, where the decay $\pi \to qq$ is possible. When $m_\sigma = 2m_\pi$ the temperature is the dissociation temperature, $T_{\rm diss}$, where the $\sigma \to \pi\pi$ decay can occur. In the chiral limit, $T_{\rm Mott} = T_{\rm diss} = T_C$. When $T > T_{\rm diss}$, a σ meson can decay into two π mesons. When $T > T_{\rm Mott}$, a π meson can decay into a pair of positive and negative quarks. When the temperature is $T_{\rm Mott}$, there is a distinct transition in m_π. There is also a distinct transition from $m_\sigma > 2m_\pi$ to $m_\sigma \approx 2m_\pi$ at $T_{\rm Mott}$. So we set $T_{\rm Mott} \approx T_{\rm diss}$ in our work, and for the strong magnetic field this relation is also fulfilled.

The phase transition with temperature is a crossover, and we see that in the crossover region, the mass of the σ meson increases with the increase of the magnetic field. However in the crossover region, the mass of the π_0 meson decreases slightly with the increase of magnetic field. This result agrees with that in Ref. [43]. When chiral symmetry is restored, the mass of the σ meson is degenerate with that of the π_0 meson. At a finite temperature, the mass of the constituent quarks increase with the enhancement of the magnetic field, due to the fact that the external magnetic field can also cause magnetic catalysis (MC) [44-46]. In Fig. 2, we can clearly see that T_C and $T_{\rm Mott}$ are all increasing, and when the magnetic field is strong enough, $T_{\rm Mott} \approx T_C$.

Figure 3 shows the diagrams of mass change corresponding to the temperature under different chemical potentials $\mu = 0,100,200,300$ MeV, where we fix the magnetic filed $eB = 5m_\pi^2$. From these figures, it is observed that when the temperature increases, the mass of the quarks decreases slowly and then decreases quickly. Finally the mass of quark changes slowly around $T = 200,190,160,90$ MeV and tends to stay unchanged for different

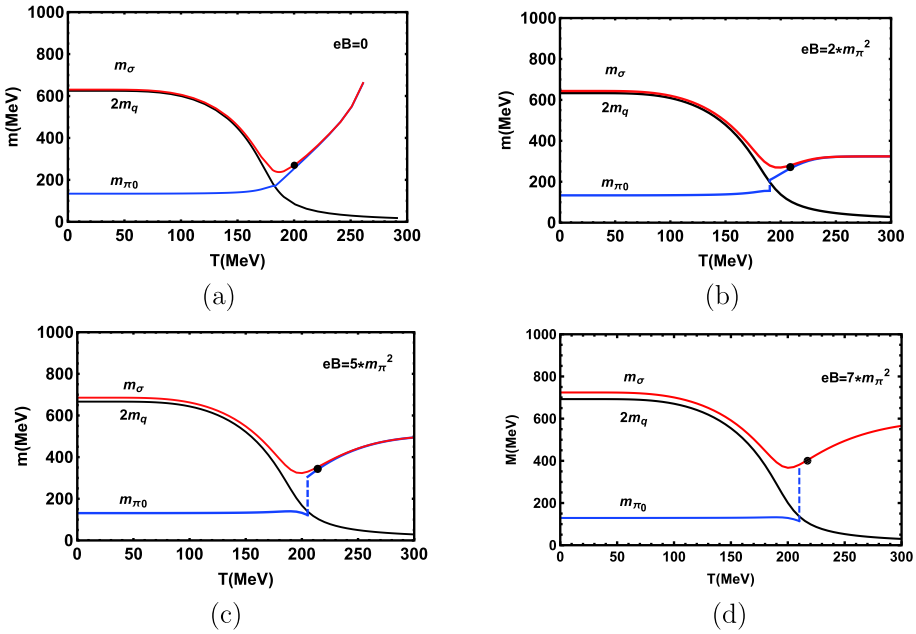

Fig. 2. (color online) Masses of quarks, σ and π_0 mesons at $eB = 0,2,5,7m_\pi^2$ when $\mu = 0$.

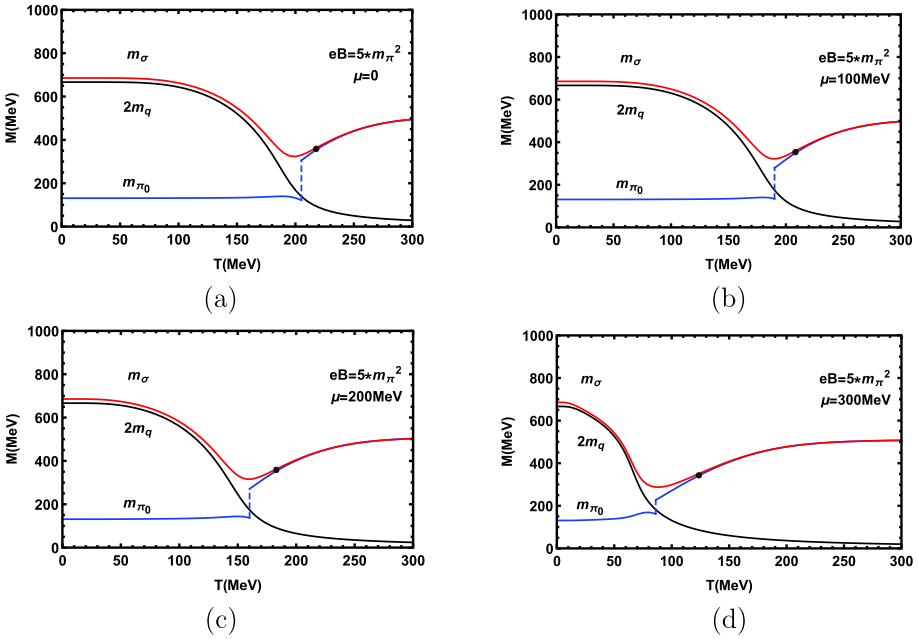

Fig. 3. (color online) Masses of quark σ and π_0 mesons at $\mu = 0, 100, 200, 300$ MeV when $eB = 5m_\pi^2$.

chemical potentials. For a fixed temperature, we find that as the chemical potential increases, the mass of quark gradually decreases.

When chiral symmetry is restored, the mass of the σ meson degenerates to the mass of the π_0 meson. Here one can clearly observe that for a fixed strong external magnetic field, with increasing chemical potential, the Mott transition temperature $T_{\rm Mott}$ and the critical temperature $T_{\rm C}$ for the restoration of chiral symmetry are both decreasing gradually. In the crossover region, the mass of the σ meson decreases continually with the chemical potential, while the mass of the π_0 increases with the chemical potential. There is still a sharp change in the mass of π_0 for the existence of the magnetic field.

In fact, there is some non-monotonical behavior of the pion mass near the critical temperature, which does not conflict with the chiral symmetry restoration process. This behavior was predicted by Son and Stephanov in Ref. [47] by scaling and universality arguments, and also observed later by the lattice results in Ref. [48]. This behavior is due to the interplay between the pion's velocity and its screening mass at finite temperature. The pion's velocity drops near $T_{\rm C}$, while the screening mass increases with temperature.

Figure 4 shows the corresponding coupling constants $g_{\pi_0 qq}$ and $g_{\sigma qq}$ as we change the temperature. Here we fix the chemical potential $\mu = 0$ and the magnetic fields are $eB = 0, 2, 5, 7m_\pi^2$. One can see that the coupling constant becomes larger with the increase of the magnetic field. For a fixed magnetic field, the coupling constant is basically constant at low temperature, then it changes significantly around $T = 200$ MeV.

In Fig. 4 (a), the corresponding coupling constant $g_{\pi_0 qq}$ increases slightly with the increase of magnetic field when we choose a fixed temperature. In Fig. 4 (b), the corresponding coupling constant $g_{\sigma qq}$ also increases with the increase of magnetic field. When it reaches $T_{\rm Mott}$, $g_{\pi_0 qq}$ drops down significantly and then jumps to a high value.

Figure 5 shows the effects of the chemical potential through coupling constants $g_{\pi_0 qq}$ and $g_{\sigma qq}$. Here we fix the magnetic field $eB = 5m_\pi^2$ and the chemical potentials are $\mu = 0, 100, 200, 300$ MeV. In Fig. 5 (a), the coupling constant becomes smaller with the increase of chemical potential. For a fixed magnetic field, the coupling constant is basically constant and then changes significantly when the chemical potential is finite. One can clearly see that the critical temperature when $g_{\pi_0 qq}$ jumps is decreasing with the increase of chemical potential, which means adding chemical potential suppresses the decay of the π_0 meson. In Fig. 5 (b), the chemical potential has a significant impact on coupling constant $g_{\sigma qq}$, and it decreases gradually with the increase of temperature.

The variation of the decay width $\Gamma_{\sigma\to\pi_0\pi_0}$ with temperature is shown in Fig. 6 and Fig. 7. We fix the chemical potential $\mu = 0$ in Fig. 6, and the magnetic fields are respectively $eB = 0, 2, 5, 7m_\pi^2$. We find that when the magnetic field increases, the decay width increases. In Lattice QCD [49], the decay widths of π_0 have been calculated. The decay constant also shows an increase with the increase of magnetic field. When $eB = 0$, the decay width is 84.7 MeV, and when the magnetic field is added, the decay width becomes 153.1, 310.2, and 510.6 MeV respectively. This is about 1.8 times, 3.7 times and 6.0 times of that in the case of zero magnetic field. With the increase of temperature, the decay critical point also in-

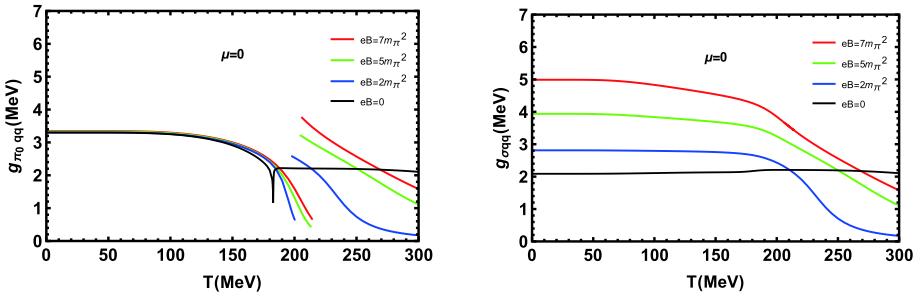

Fig. 4. (color online) Coupling constants $g_{\pi_0 qq}$ and $g_{\sigma qq}$ at different magnetic fields when the chemical potential $\mu = 0$.

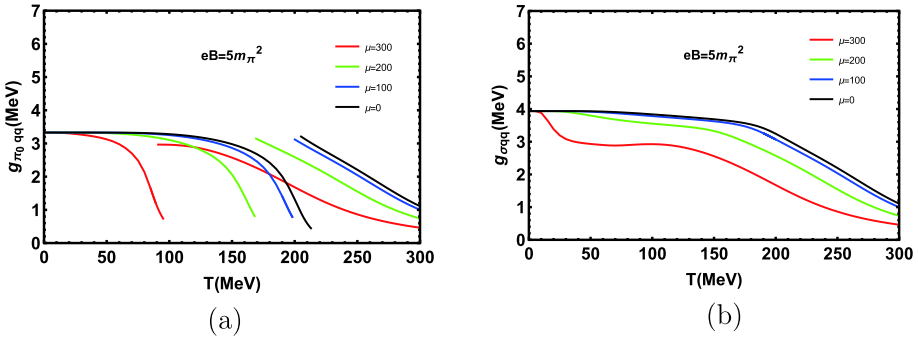

Fig. 5. (color online) Coupling constants $g_{\pi_0 qq}$ and $g_{\sigma qq}$ at different chemical potentials when the magnetic field $eB = 5m_\pi^2$.

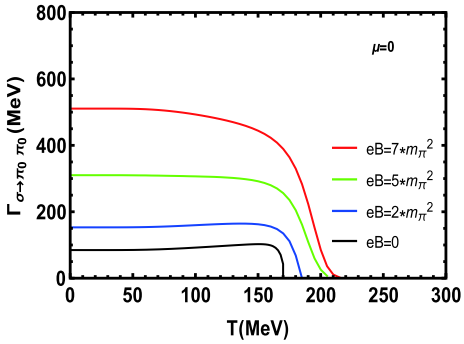

Fig. 6. (color online) Decay width $\Gamma_{\sigma\to\pi_0\pi_0}$ at different magnetic fields when the chemical potential $\mu = 0$.

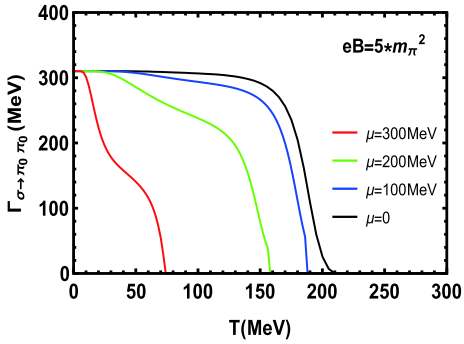

Fig. 7. (color online) Decay width $\Gamma_{\sigma\to\pi_0\pi_0}$ at different chemical potentials when the magnetic field $eB = 5m_\pi^2$.

creases from $T = 170$ MeV to $T = 220$ MeV. Finally the decay width $\Gamma_{\sigma\to\pi_0\pi_0}$ decreases, and goes to 0 when the temperature is around the critical point temperature. At this temperature, the decay happens rapidly and then stops.

In Fig. 7 we fix the magnetic field $eB = 5m_\pi^2$, and the chemical potentials are $\mu = 0, 100, 200, 300$ MeV. One find that when the chemical potential increases, the corresponding decay width $\Gamma_{\sigma\to\pi_0\pi_0}$ decreases, and the decay critical points move to lower temperature. Their temperatures are respectively 210, 189, 159, 72 MeV. Near to the critical point, $\Gamma_{\sigma\to\pi_0\pi_0}$ suddenly changes to 0, which means the decay process stops. It is clear that the presence of the chemical potential suppresses the decay of σ meson.

Under the corresponding magnetic field in Fig. 6, the decay width increases with the increase of magnetic field, and it drops to zero at $T_{\rm Mott}$, which reflects the restoration of chiral symmetry. Similar results on the decay widths of σ mesons at fixed chemical potential $\mu = 0$ can be found in Ref. [50] for the study of the decay widths of neutral π mesons decaying into photons for different neutral mesons. The increase of decay width is particularly pronounced when the magnetic field is very large. When we consider different chemical potentials and fix the external magnetic field $eB = 5m_\pi^2$ in Fig. 7, the change of $\Gamma_{\sigma\to\pi_0\pi_0}$ looks very clear and the critical point decreases with the chemical potential.

In Ref. [5], they have considered the weak decay constant of π_0 at finite temperature T, chemical potential μ

and in the presence of a constant magnetic field B. In their work, they consider the decay constant of π_0 at $\mu = 0$. In our paper, we mainly calculate the decay constant of σ with different chemical potentials and magnetic fields, that is the new point in our paper. We also calculate the mass spectra of mesons.

From all the figures, one may find that the critical temperature of $g_{\pi_0 qq}$, $g_{\sigma qq}$ and $\Gamma_{\sigma\to\pi_0\pi_0}$ is $T_{\rm Mott}$, not $T_{\rm C}$. In Refs. [27, 38, 39], $\Gamma_{\sigma\to\pi\pi}$ is usually associated with the chiral phase transition. In their work, the threshold temperature is $T_{\rm diss}$ since there is no magnetic field. With the magnetic field, $T_{\rm C}$ and $T_{\rm Mott}$ are different — this difference is studied in Refs. [34-36]. $T_{\rm Mott}$ is decreasing with the increase of chemical potential, which agrees with Ref. [38]. In that paper, $\Gamma_{\rm max}$ is first decreasing and then increasing with the increase of chemical potential, and when the chemical potential is bigger enough, it turns to zero. In our work, the change of $\Gamma_{\sigma\to\pi_0\pi_0}$ is different since we chose a constant magnetic field $eB = 5m_\pi^2$. With the increase of chemical potential, $\Gamma_{\sigma\to\pi_0\pi_0}$ is clearly decreasing.

V. SUMMARY AND CONCLUSION

Magnetic fields were generated in the early universe. They can influence subsequent cosmic phase transitions, which is important for particle physics in the early universe. Our results suggest that the presence of an external magnetic field "magnetizes" quarks in neutral mesons, affecting their thermodynamic properties. The existence of the magnetic field increases the critical temperature, thus increasing the symmetry breaking region and suppressing the phase transition to some extent.

From this work, we clearly see that the neutral meson is also affected by the external magnetic field, which is mainly due to the "magnetization" of the charged quarks that make up the meson, which affects the properties of the meson, such as meson mass, coupling constant, decay width and so on. Here, the effect of the magnetic field is to increase the critical temperature in the mass spectrum, thereby increasing the symmetry breaking region. At the same time, the existence of the magnetic field breaks the isospin symmetry, and the separation of quark energy levels leads to the jump in π_0 mass.

The effect of the chemical potential is to decrease the critical temperature in the mass spectrum. In the case of fixed strong external magnetic field $eB = 5m_\pi^2$, with the increase of chemical potential, the masses of σ, π_0 and quark don't change much at low temperature, while the coupling constants and decay width all decrease. The existence of chemical potential reduces the critical temperature and accelerates the restoration of chiral symmetry. It is worth mentioning that the critical temperature of $g_{\pi_0 qq}$, $g_{\sigma qq}$ and $\Gamma_{\sigma\to\pi_0\pi_0}$ is $T_{\rm Mott}$, not $T_{\rm C}$. We know that the truly critical temperature of $\sigma\to\pi_0\pi_0$ should be $T_{\rm diss}$, and $T_{\rm Mott}\approx T_{\rm diss}$ when we consider the magnetic field in our work.

To conclude, we use $SU(2)$ NJL model to study the decay process of $\sigma\to\pi_0\pi_0$, and our results show that the magnetic field will enhance the decay process while the chemical potential will reduce the decay process. In this work, a general method is used to calculate the decay constant, which can be extended to other charged mesons, such as K or ρ mesons. It can also be extended to other backgrounds, such as the 3-flavor NJL model, PNJL model and so on.

References

[1] M. L. Goldberger and S. B. Treiman, Phys. Rev. **110**, 1178 (1958)
[2] M. Gell-Mann, R. J. Oakes, and B. Renner, Phys. Rev. **175**, 2195 (1968)
[3] O. Soloveva, P. Moreau, and E. Bratkovskaya, Phys. Rev. C **101**, 045203 (2020), arXiv:1911.08547
[4] S. Fayazbakhsh, S. Sadeghian, and N. Sadooghi, Phys. Rev. D **86**, 085042 (2012), arXiv:1206.6051[hep-ph]
[5] S. Fayazbakhsh and N. Sadooghi, Phys. Rev. D **88**(6), 065030 (2013), arXiv:1306.2098[hep-ph]
[6] S. Fayazbakhsh and N. Sadooghi, PoS Confinement X, 294 (2012), arXiv:1302.0622[hep-ph]
[7] F. Kayanikhoo, K. Naficy, and G. H. Bordbar, Eur. Phys. J. A **56**, 2 (2020), arXiv:1911.10512
[8] Z. Gong, F. Mackenroth, X. Q. Yan *et al.*, Sci. Rep. **9**(1), 17181 (2019)
[9] K. Xu, J. Chao, and M. Huang, Phys. Rev. D **103**, 076015 (2021), arXiv:2007.13122 [hep-ph]
[10] K. Xu, S. Shi, H. Zhang *et al.*, Phys. Lett. B **809**, 135706 (2020), arXiv:2004.05362 [hep-ph]
[11] J. O. Andersen, W. R. Naylor, and A. Tranberg, Rev. Mod. Phys. **88**, 025001 (2016), arXiv:1411.7176[hep-ph]
[12] V. A. Miransky and I. A. Shovkovy, Phys. Rept. **576**, 1 (2015), arXiv:1503.00732[hep-ph]
[13] H. Li, X. l. Sheng, and Q. Wang, Phys. Rev. C **94**(4), 044903 (2016), arXiv:1602.02223[nucl-th]
[14] I. Siddique, X. L. Sheng, and Q. Wang, Phys. Rev. C **104**, 034907 (2021), arXiv:2106.00478
[15] I. V. Selyuzhenkov, (STAR Collaboration), Rom. Rep. Phys. **58**, 049 (2006) [nucl-ex/0510069]
[16] D. E. Kharzeev, L. D. McLerran, and H. J. Warringa, Nucl. Phys. A **803**, 227 (2008), arXiv:0711.0950[hep-ph]
[17] V. Skokov, A. Y. Illarionov, and V. Toneev, Int. J. Mod. Phys. A **24**, 5925 (2009), arXiv:0907.1396[nucl-th]
[18] E. J. Ferrer, V. de la Incera, J. P. Keith *et al.*, Phys. Rev. C **82**, 065802 (2010), arXiv:1009.3521[hep-ph]
[19] A. Ayala, P. Amore, and A. Aranda, Phys. Rev. C **66**, 045205 (2002), arXiv:hep-ph/0207081
[20] Y. Nambu and G. Jona-Lasinio, Phys. Rev. **124**, 246 (1961)
[21] S. P. Klevansky, Rev. Mod. Phys. **64**, 649 (1992)
[22] T. Hatsuda and T. Kunihiro, Phys. Rept. **247**, 221 (1994), arXiv:hep-ph/9401310

[23] M. Buballa, Phys. Rept. **407**, 205 (2005), arXiv:hep-ph/0402234
[24] Joseph I. Kapusta and Charles Gale. *Finite-Temperature Field Theory: Principles and Applications*. Cambridge Monographs on Mathematical Physics. Cambridge University Press, 2 edition, 2006
[25] Teiji Kunihiro and Tetsuo Hatsuda, Physics Letters B **206**(3), 385-390 (1988)
[26] Yoichiro Nambu and G. Jona-Lasinio, Phys. Rev. **122**, 345-358 (1961)
[27] P. Zhuang, J. Hufner, and S. P. Klevansky, Nucl. Phys. A **576**, 525 (1994)
[28] V. I. Ritus, Annals Phys. **69**, 555 (1972)
[29] V. I. Ritus, Sov. Phys. JETP **48**, 788 (1978) [Zh. Eksp. Teor. Fiz. **75**, 1560 (1978)]
[30] C. N. Leung and S. Y. Wang, Nucl. Phys. B **747**, 266 (2006), arXiv:hep-ph/0510066
[31] E. Elizalde, E. J. Ferrer, and V. de la Incera, Annals Phys. **295**, 33 (2002), arXiv:hep-ph/000703
[32] D. P. Menezes, M. Benghi Pinto, S. S. Avancini *et al*., Phys. Rev. C **79**, 035807 (2009), arXiv:0811.3361[nucl-th]
[33] K. Fukushima, D. E. Kharzeev, and H. J. Warringa, Nucl. Phys. A **836**, 311 (2010), arXiv:0912.2961[hep-ph]
[34] S. Mao, Phys. Rev. D **94**(3), 036007 (2016), arXiv:1605.04526[hep-th]
[35] S. Mao, Phys.Rev.D **96**(3), 034004 (2017)
[36] S. Mao, Chin. Phys. C **45**(2), 021004 (2021), arXiv:1908.02851
[37] S. Mao, Phys. Rev. D **99**(5), 056005 (2019), arXiv:1808.10242[nucl-th]
[38] X. Zhu and P. Zhuang, Commun. Theor. Phys. **37**, 431-434 (2002), arXiv:nucl-th/0110039[nucl-th]
[39] P. Zhuang and Z. Yang, Chin. Phys. Lett. **18**, 344-346 (2001), arXiv:nucl-th/0008041[nucl-th]
[40] R. Gatto and M. Ruggieri, Lect. Notes Phys. **871**, 87 (2013), arXiv:1207.3190[hep-ph]
[41] F. Preis, A. Rebhan, and A. Schmitt, Lect. Notes Phys. **871**, 51 (2013), arXiv:1208.0536[hep-ph]
[42] S. Mao, Phys. Lett. B **758**, 195-199 (2016), arXiv:1602.06503[hep-ph]
[43] F. Preis, A. Rebhan, and A. Schmitt, JHEP **1103**, 033 (2011), arXiv:1012.4785[hep-th]
[44] T. Inagaki, D. Kimura, and T. Murata, Prog. Theor. Phys. **111**, 371 (2004), arXiv:hep-ph/0312005
[45] K. G. Klimenko, Z. Phys. C **54**, 323 (1992)
[46] V. P. Gusynin, V. A. Miransky, and I. A. Shovkovy, Nucl. Phys. B **462**, 249 (1996), arXiv:hep-ph/9509320
[47] D. T. Son and M. A. Stephanov, Phys. Rev. Lett. **88**, 202302 (2002), arXiv:hep-ph/0111100[hep-ph]
[48] B. B. Brandt, A. Francis, H. B. Meyer *et al*., Phys. Rev. D **90**(5), 054509 (2014), arXiv:1406.5602[hep-lat]
[49] H. T. Ding, S. T. Li, A. Tomiya *et al*., Phys. Rev. D **104**(1), 014505 (2021), arXiv:2008.00493[hep-lat]
[50] P. Costa, M. C. Ruivo, and Y. L. Kalinovsky, Phys. Rev. C **70**, 048202 (2004), arXiv:hep-ph/0403263